Electronic Supplementary Information

Polydiphenylamine as a promising high-energy cathode material for dual-ion batteries

Filipp A. Obrezkov,[a]* Alexander F. Shestakov,[b] Sergey G. Vasil'ev,[b] Keith J. Stevenson[a] and Pavel A. Troshin[a,b]

[a]Center for Energy Science and Technology, Skolkovo Institute of Science and Technology, Nobel St. 3, Moscow 143026, Russia.

[b]Institute for Problems of Chemical Physics of Russian Academy of Sciences, Acad. Semenov ave. 1, Chernogolovka, Moscow region, 142432, Russia.

*E-mail: filipp.obrezkov@skoltech.ru

Calculations of specific capacity and energy density of $PDPAPF_6$

Specific capacity ($Q_{PDPAPF6}$) and energy density ($E_{PDPAPF6}$) of $PDPAPF_6$ were calculated by division of corresponding values obtained for PDPA (Q_{PDPA} and E_{PDPA}, respectively) by the ratio of molecular weights for monomeric units of $PDPAPF_6$ ($M._{DPAPF6}.$) and PDPA ($M._{DPA}.$) which was 1.868 (1).

$$Q_{PDPAPF6} = \frac{Q_{PDPA}}{M._{DPAPF6}./M._{DPA}.} = \frac{Q_{PDPA}}{1.868} \quad (1)$$

Similarly, specific capacities and energy densities for $PAniPF_6$ and $PTPAPF_6$ were calculated (Table S2).

Calculations of active material energy density, average discharge potential and realistic energy density of cathode composite

Experimental values of energy density were extracted from BTSDA 7.6.0.249 software which was used for the processing of the data of galvanostatic charge-discharge cycling performed using Neware BTS3000 station. The values of energy density (E) for the materials reported in literature were calculated as an area under the corresponding charge-discharge (voltage (V) vs. specific capacity (q)) curve from 0 mAh g^{-1} to the highest achieved value of specific capacity (Q) (2), if not directly stated.

$$E = \int_0^Q V dq \quad (2)$$

Average discharge potential ($V_{av.}$) was calculated by division of energy density (E) by specific capacity (Q) of the material (3).

$$V_{av.} = \frac{E}{Q} \quad (3)$$

Realistic energy density ($E_{real.}$) was calculated by multiplication of energy density (E) of active material on its content (ω) in the cathode composite (Tables S3-S4) (4).

$$E_{real.} = E * \omega \quad (4)$$

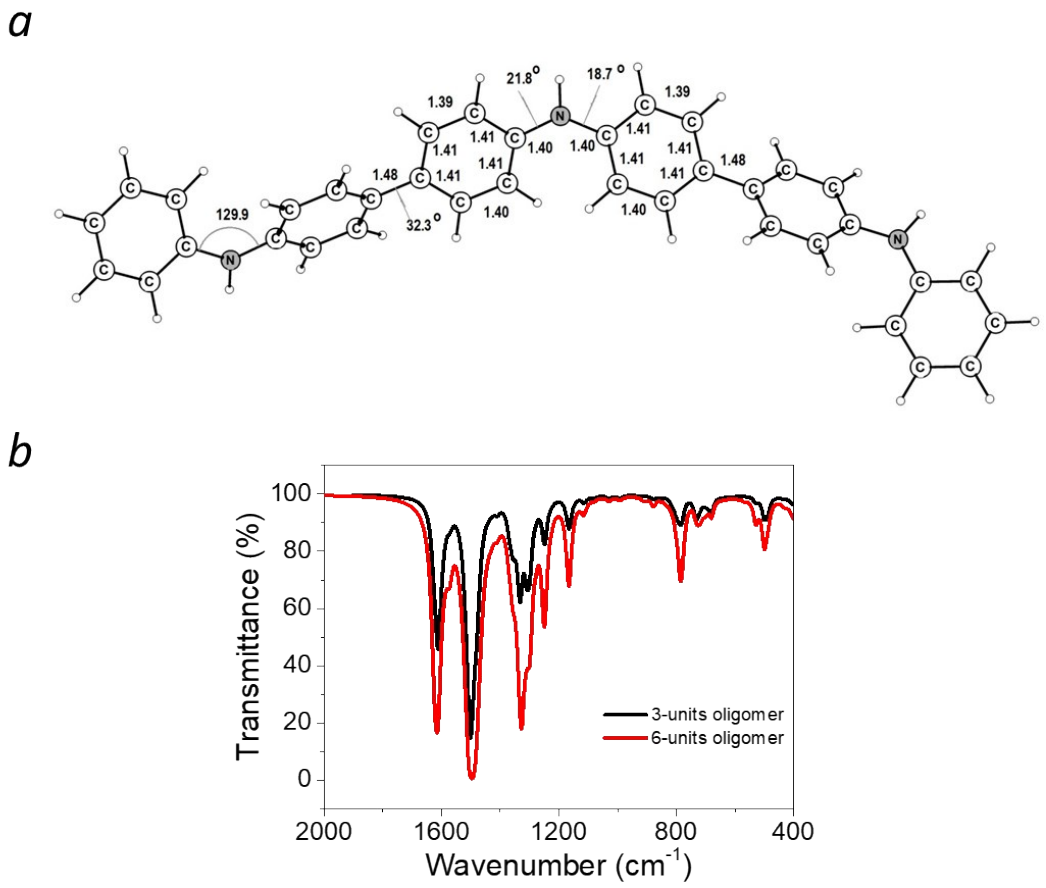

Figure S1. The DFT calculated structure of PDPA trimer (a) and comparison of the computed FTIR spectra for PDPA trimer and hexamer (b).

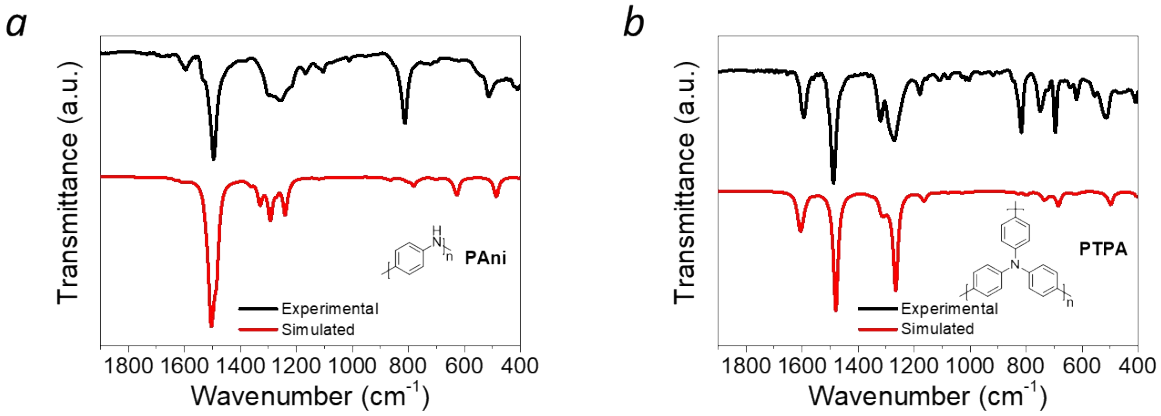

Figure S2. Comparison of the experimental and computed FTIR spectra of PAni (a) and PTPA (b).

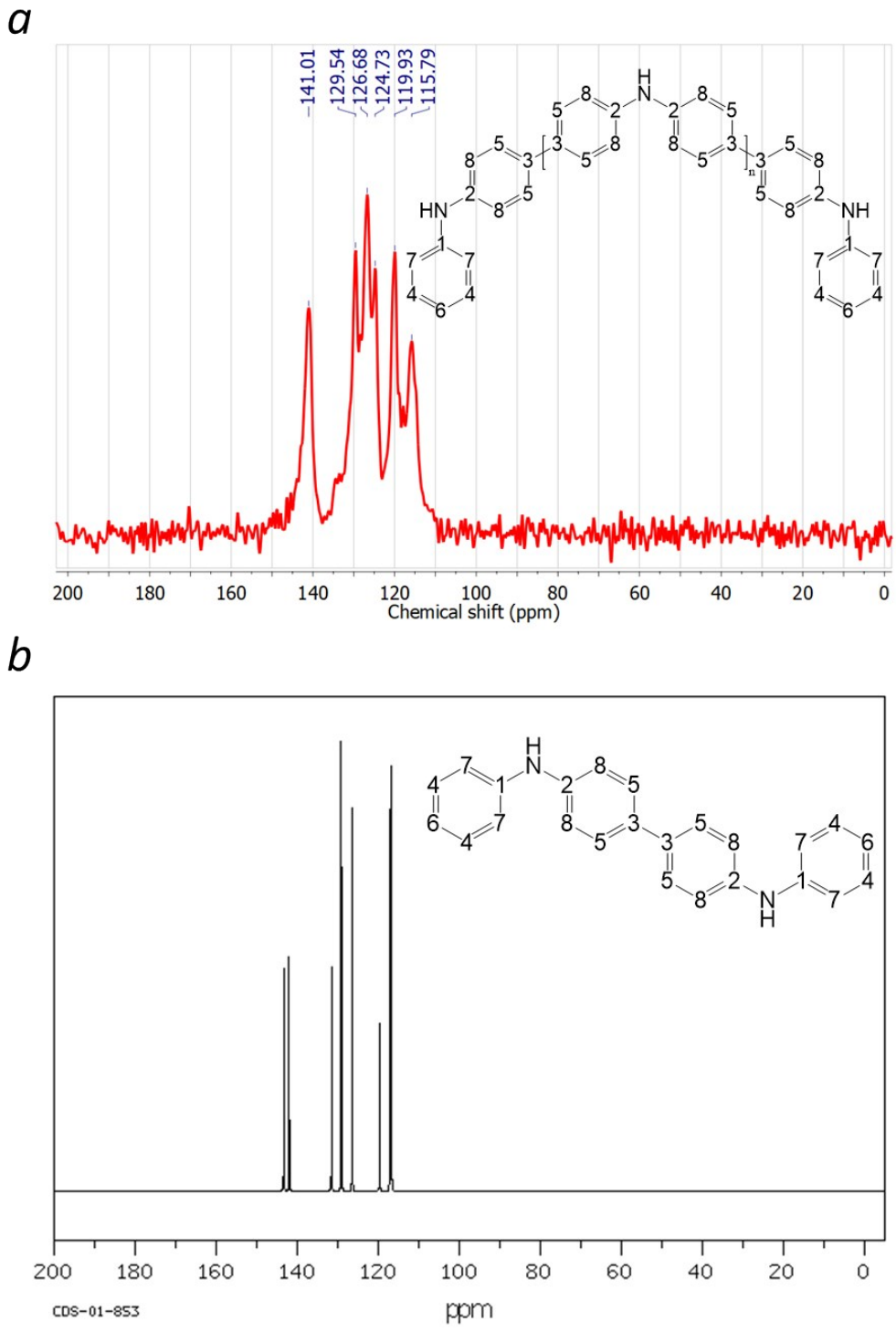

Figure S3. MAS ^{13}C ssNMR spectrum of PDPA (a) and reproduced from Spectral Database for Organic Compounds (SDBS) ^{13}C NMR spectrum of N,N'-diphenylbenzidine[1] (b).

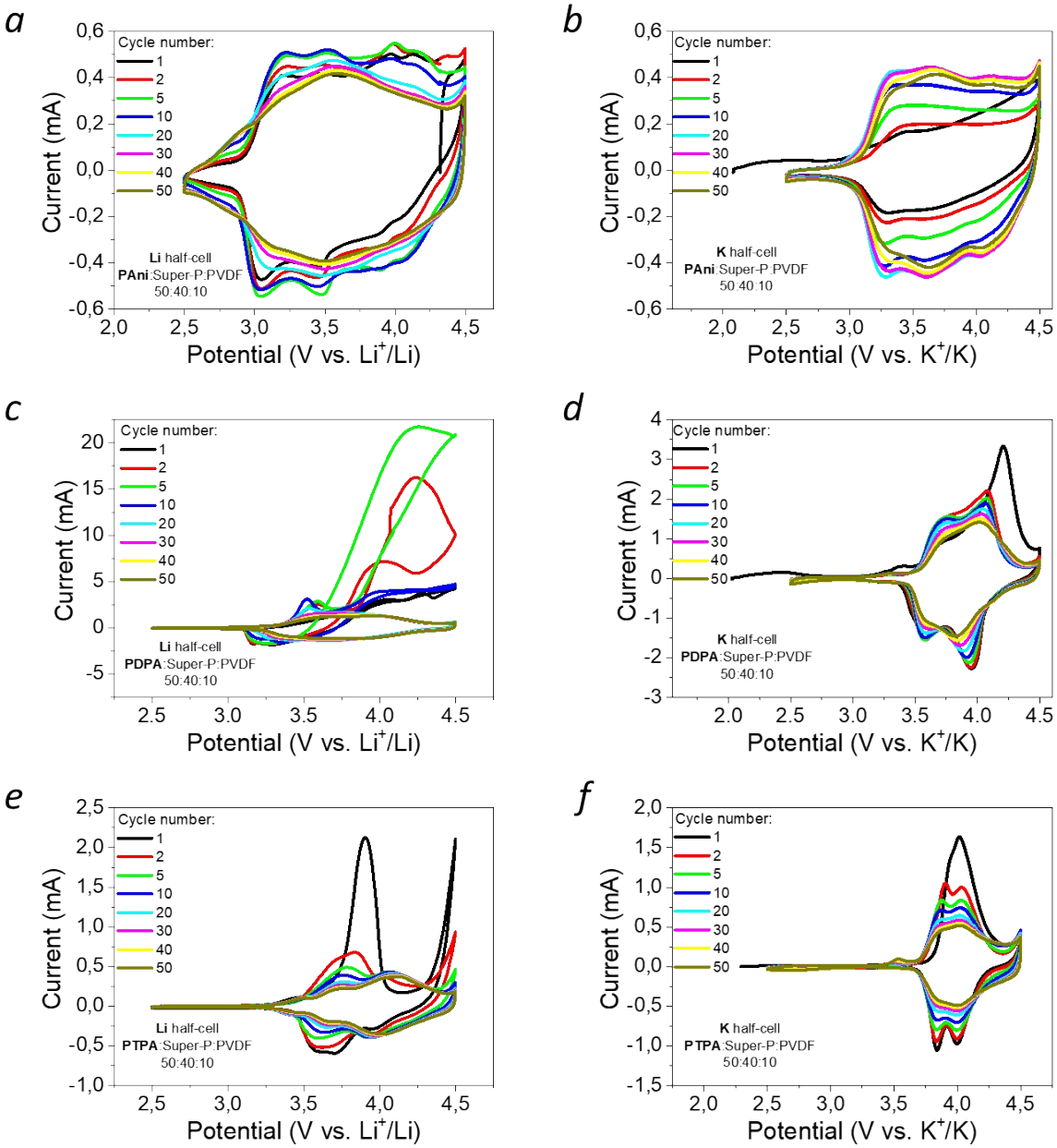

Figure S4. Cyclic voltammograms of Li (left column: a, c, e) and K (right column: b, d, f) half-cells with PAni (a, b), PDPA (c, d) and PTPA (e, f) cathode active materials.

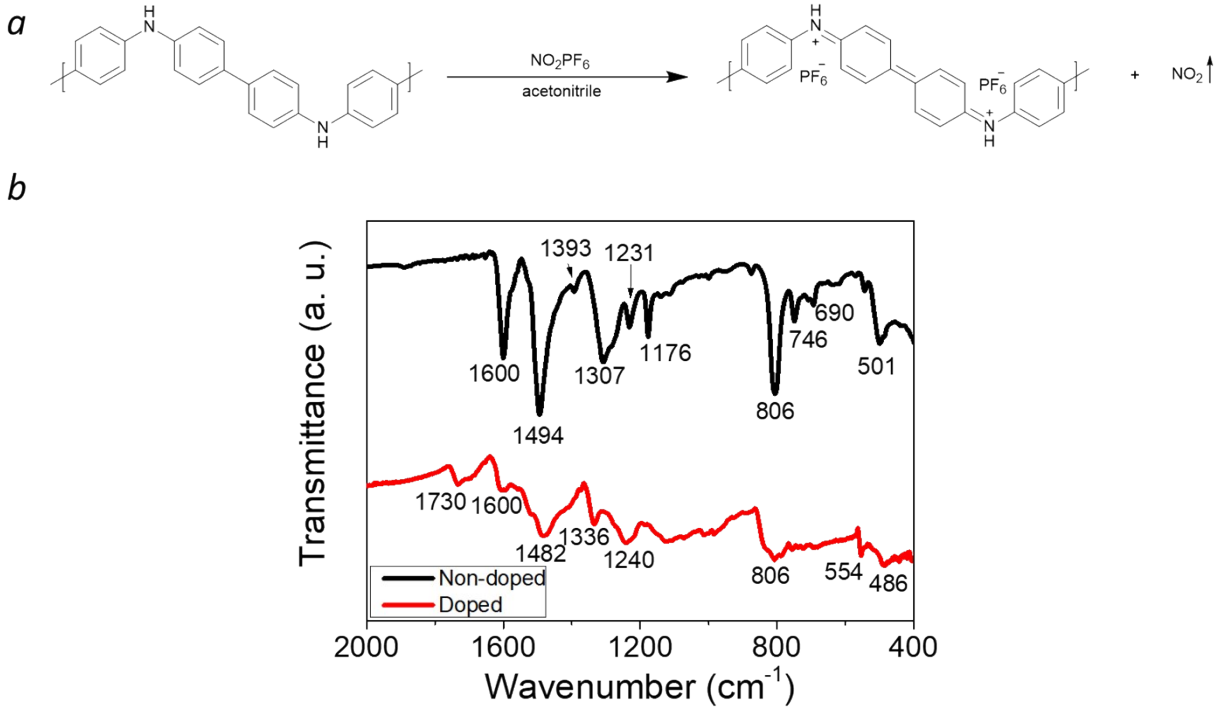

Figure S5. Reaction scheme for chemical oxidation of PDPA by 0.5M NO_2PF_6 in acetonitrile (a) and FTIR spectra of pristine (PDPA) and oxidized ($PDPAPF_6$) samples of PDPA (b).

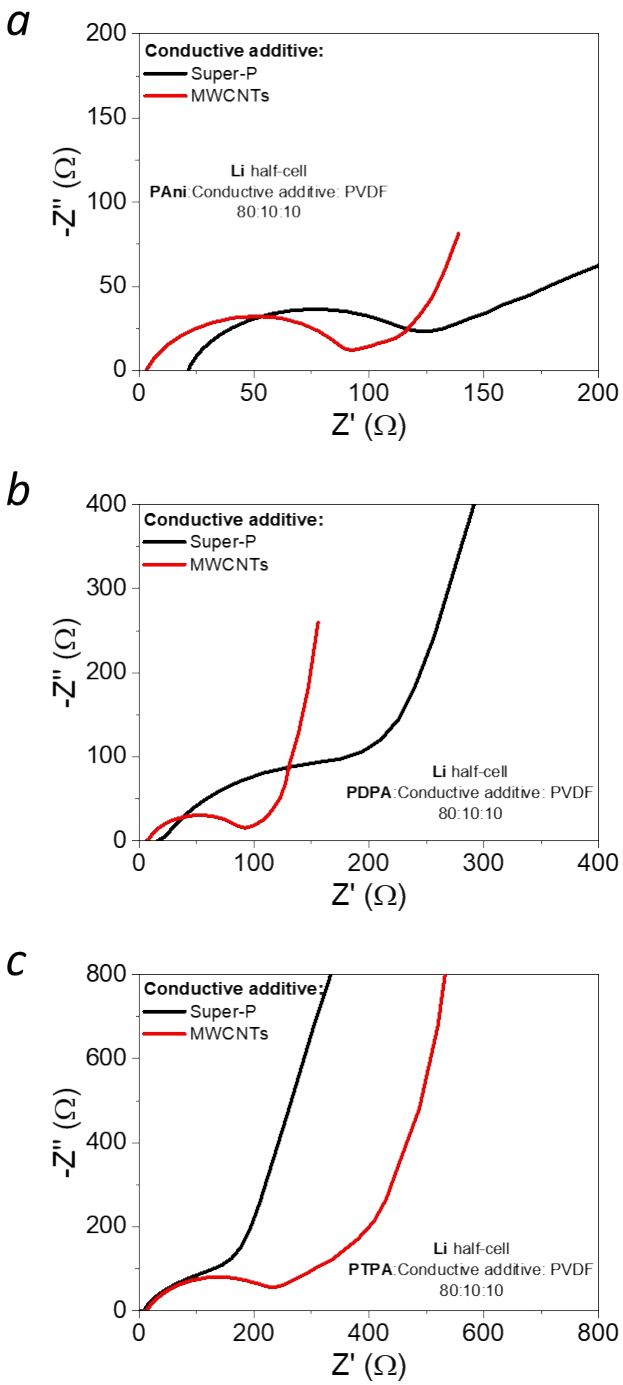

Figure S6. Electrochemical impedance spectra of Li half-cells with PAni (a), PDPA (b) and PTPA (c) cathode active materials.

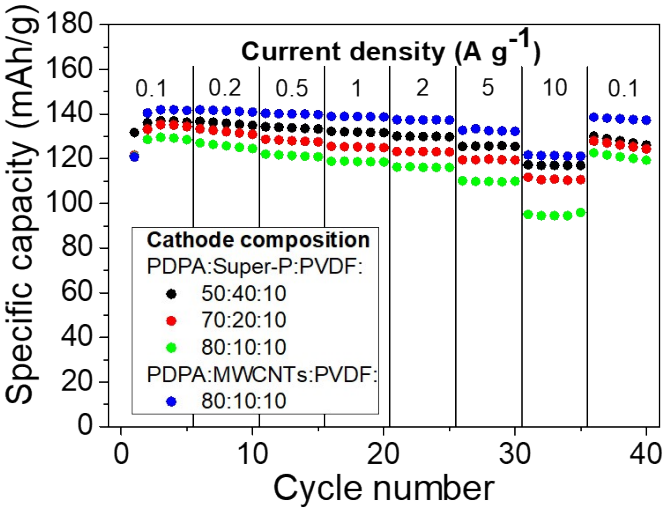

Figure S7. Capacity versus current density behavior of PDPA//Li cell with various electrode compositions.

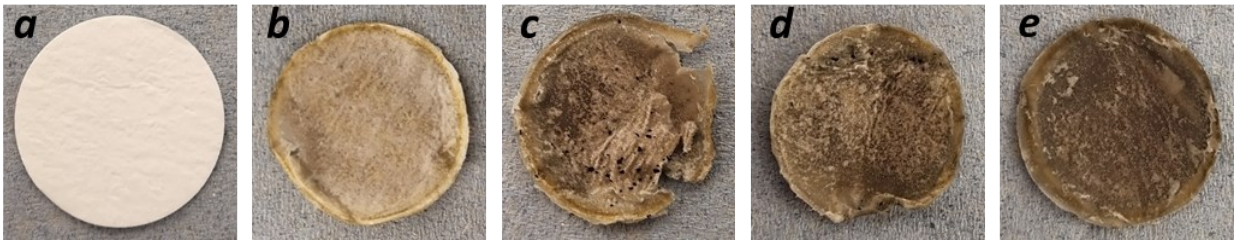

Figure S8. Appearance of the cell separator: initial state (a) and after ~100 charge-discharge cycles while composites PDPA:Super-P:PVDF (50:40:10) (b), PDPA:Super-P:PVDF (70:20:10) (c), PDPA:Super-P:PVDF (80:10:10) (d) and PDPA:MWCNTs:PVDF (80:10:10) (e) were used as cathodes.

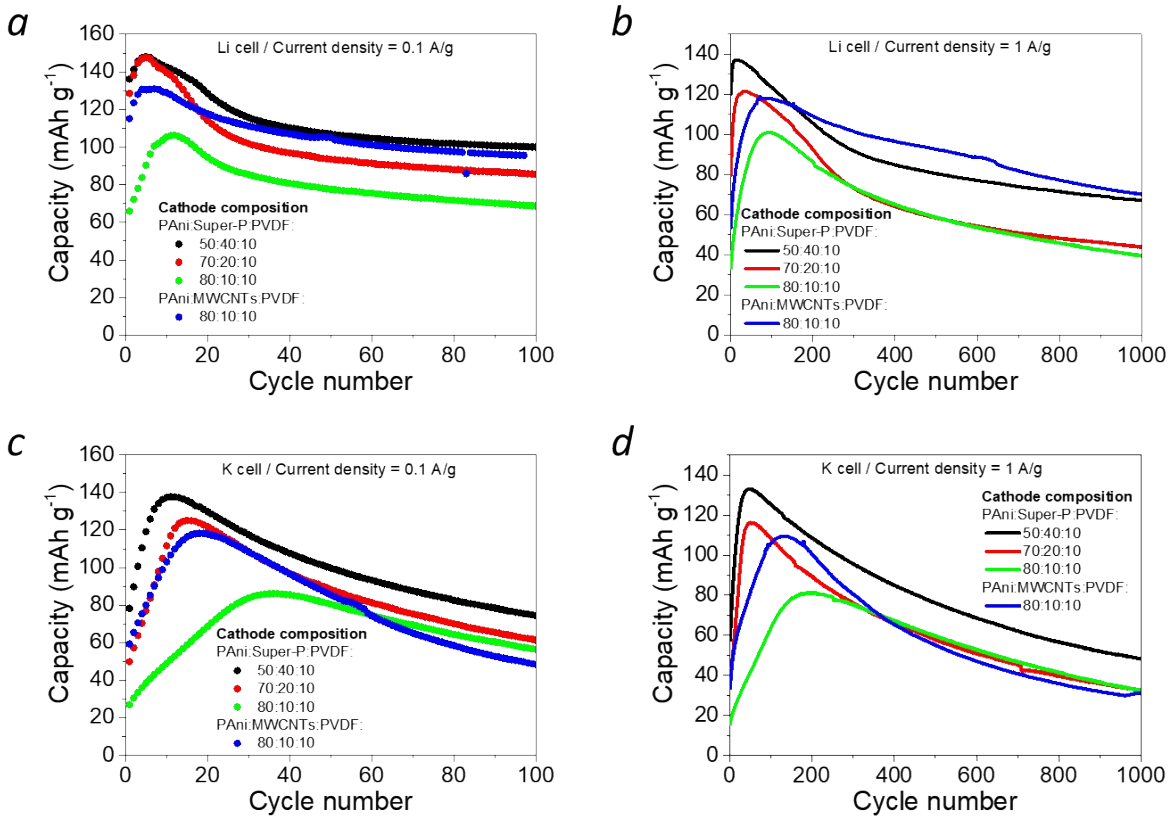

Figure S9. Evolution of specific capacity for cathodes with different composition upon charge-discharge cycling at the current density of 0.1 A g^{-1} (a, c) and 1 A g^{-1} (b, d) for lithium (a, b) and potassium (c, d) half-cells with PAni cathode active material

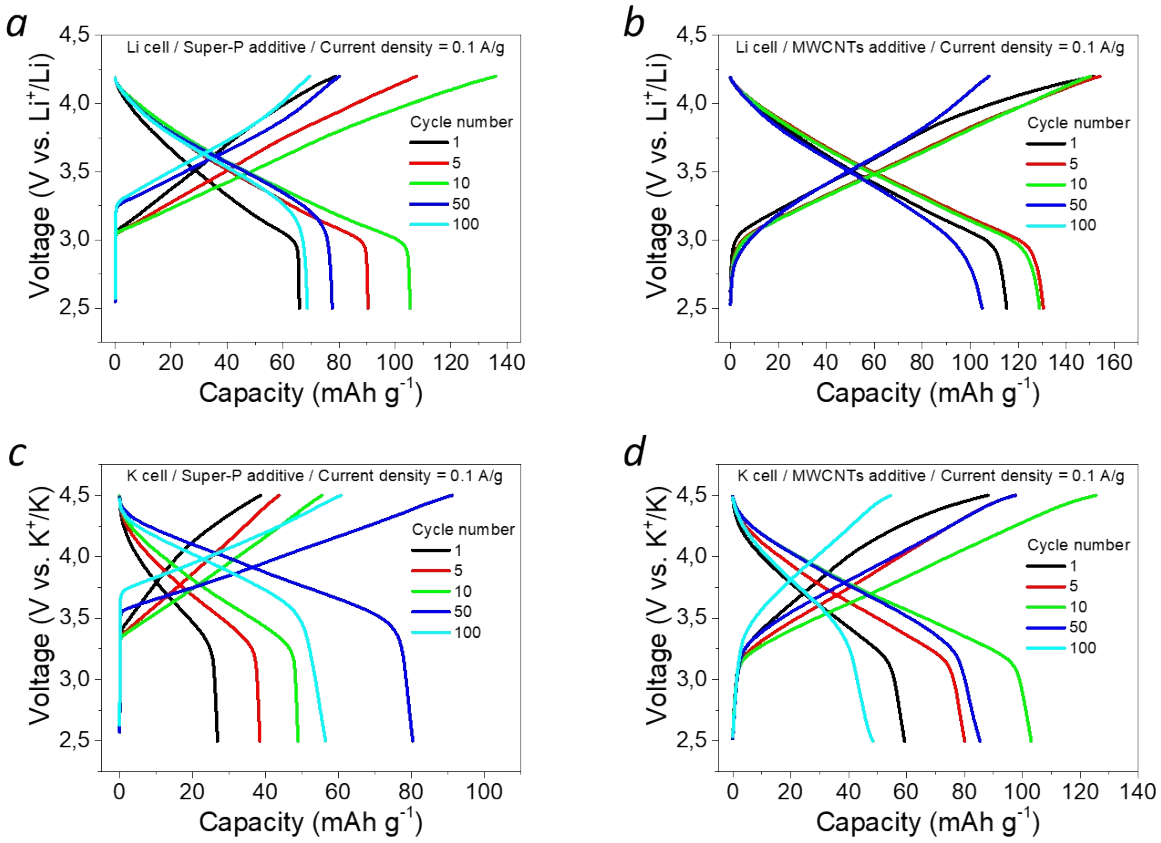

Figure S10. Charge-discharge profiles obtained at the current density of 0.1 A g^{-1} for cathode compositions PAni:conductive additive:PVDF (80:10:10) with super-P carbon (a, c) and MWCNTs (b, d) conductive additives in lithium (a, b) and potassium (c, d) half-cells.

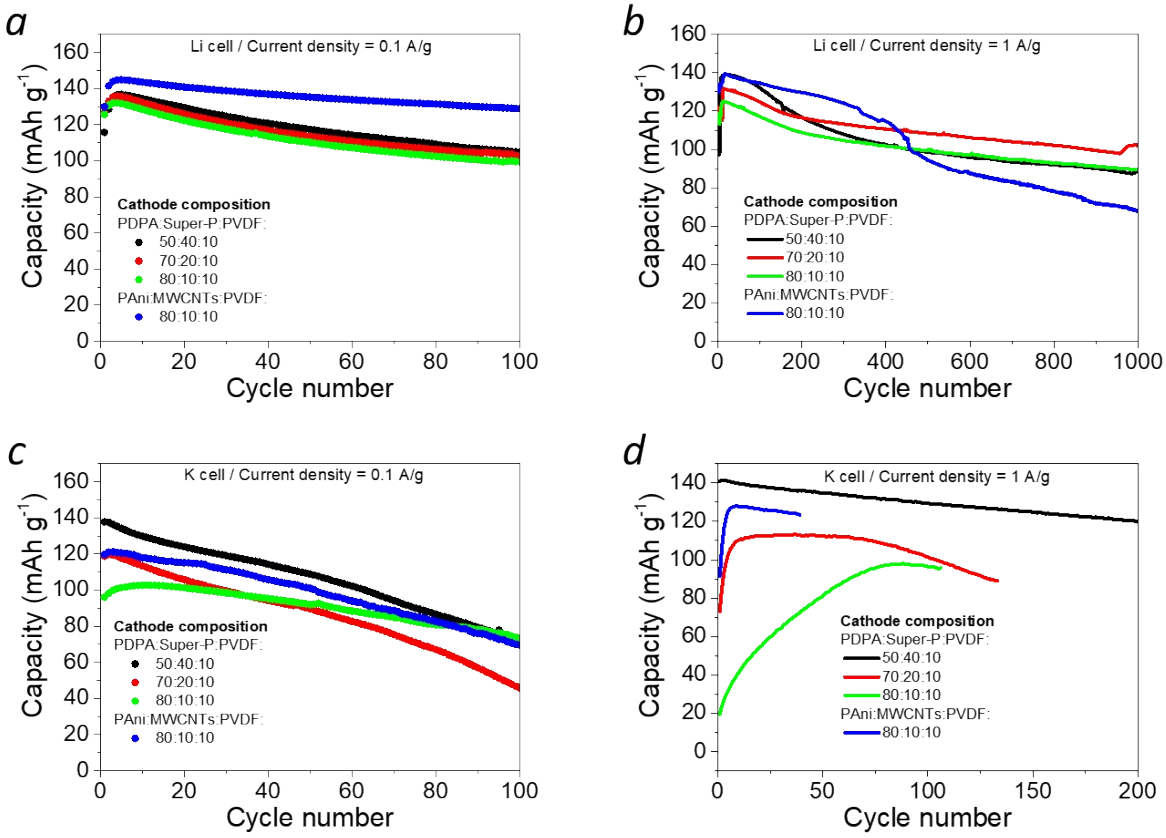

Figure S11. Evolution of specific capacity for cathodes with different composition upon charge-discharge cycling at the current density of 0.1 A g^{-1} (a, c) and 1 A g^{-1} (b, d) for lithium (a, b) and potassium (c, d) half-cells with PDPA cathode active material.

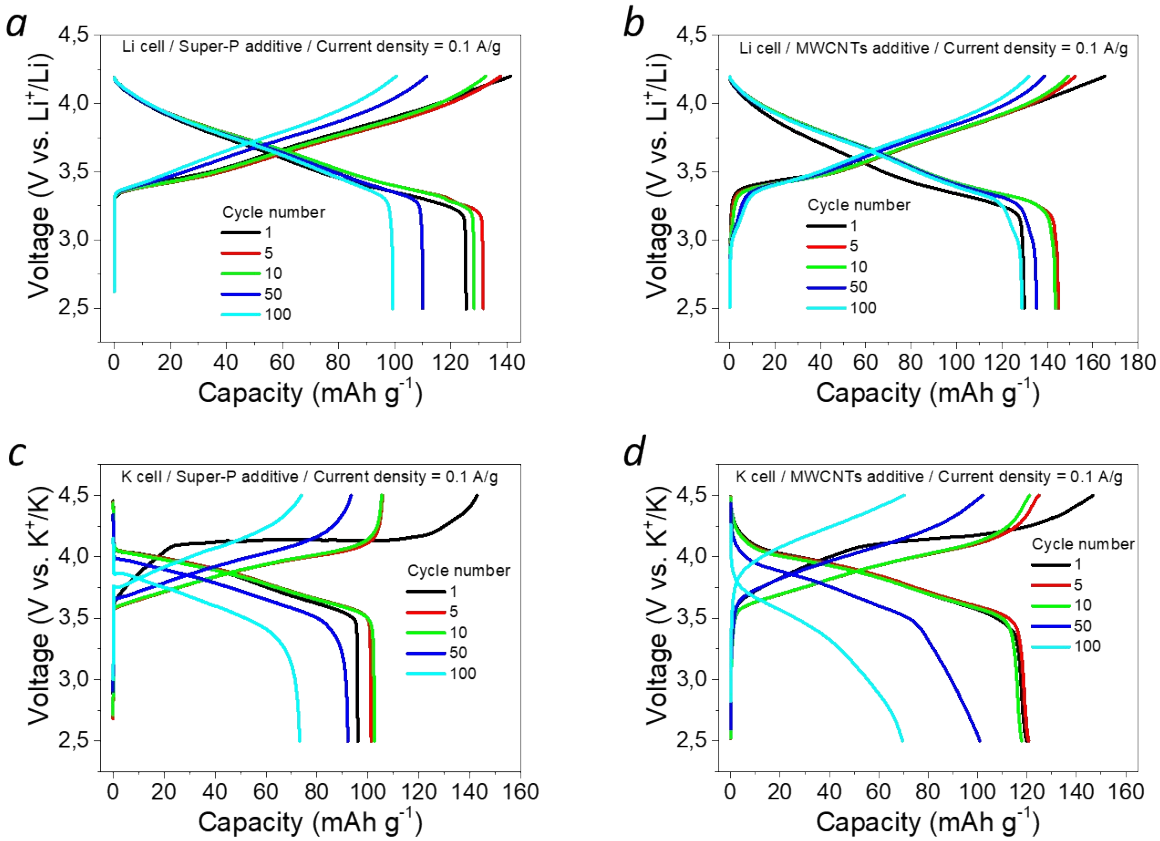

Figure S12. Charge-discharge profiles obatined at the current density of 0.1 A g^{-1} for cathode compositions PDPA:conductive additive:PVDF (80:10:10) with super-P carbon (a, c) and MWCNTs (b, d) conductive additives in lithium (a, b) and potassium (c, d) half-cells.

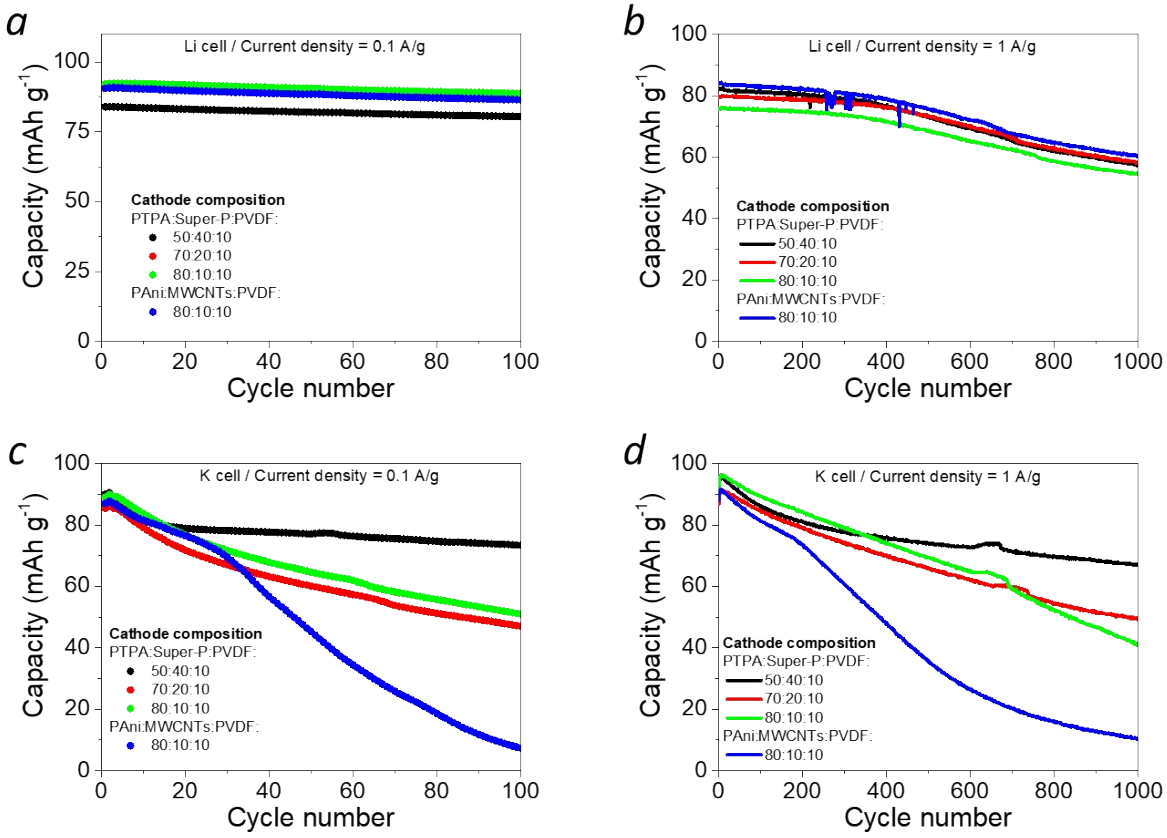

Figure S13. Evolution of specific capacity for cathodes with different composition upon charge-discharge cycling at the current density of 0.1 A g^{-1} (a, c) and 1 A g^{-1} (b, d) for lithium (a, b) and potassium (c, d) half-cells with PTPA cathode active material.

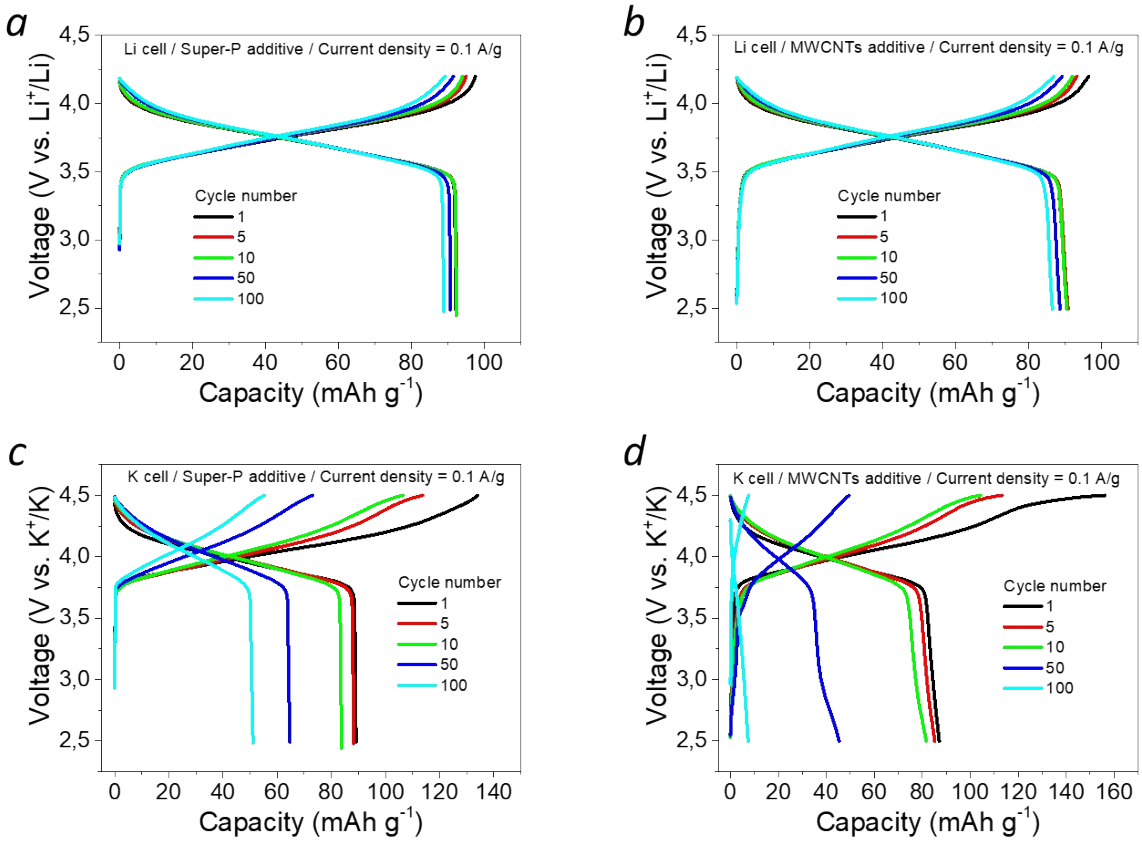

Figure S14. Charge-discharge profiles obtained at the current density of 0.1 A g^{-1} for cathode compositions PTPA:conductive additive:PVDF (80:10:10) with super-P carbon (a, c) and MWCNTs (b, d) conductive additives in lithium (a, b) and potassium (c, d) half-cells.

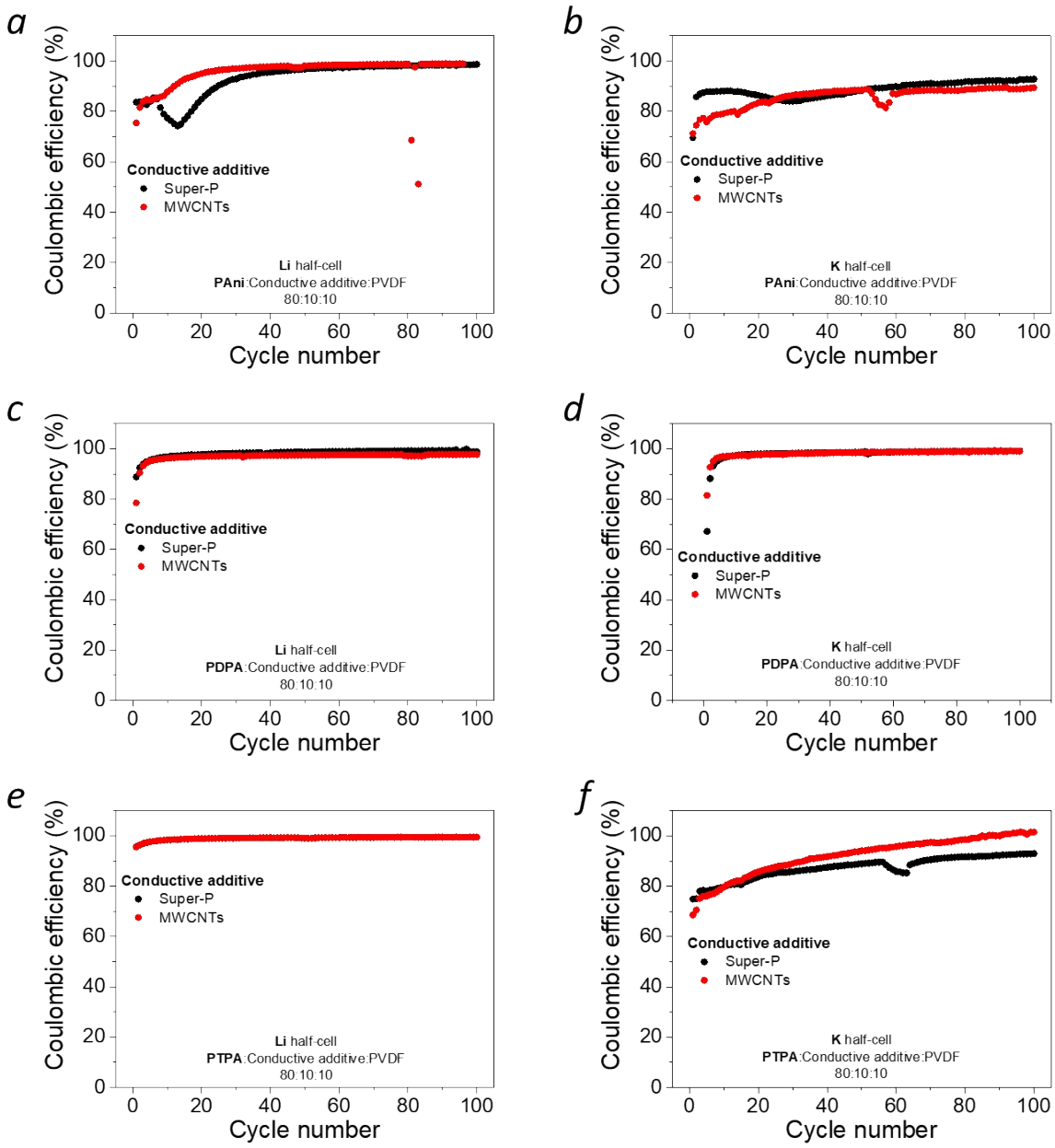

Figure S15. Evolution of the coulombic efficiencies of Li (a, c, e) and K (b, d, f) half-cells using active material:conductive additive:PVDF (80:10:10) cathodes with PAni (a, b), PDPA (c, d) and PTPA (e, f) active materials.

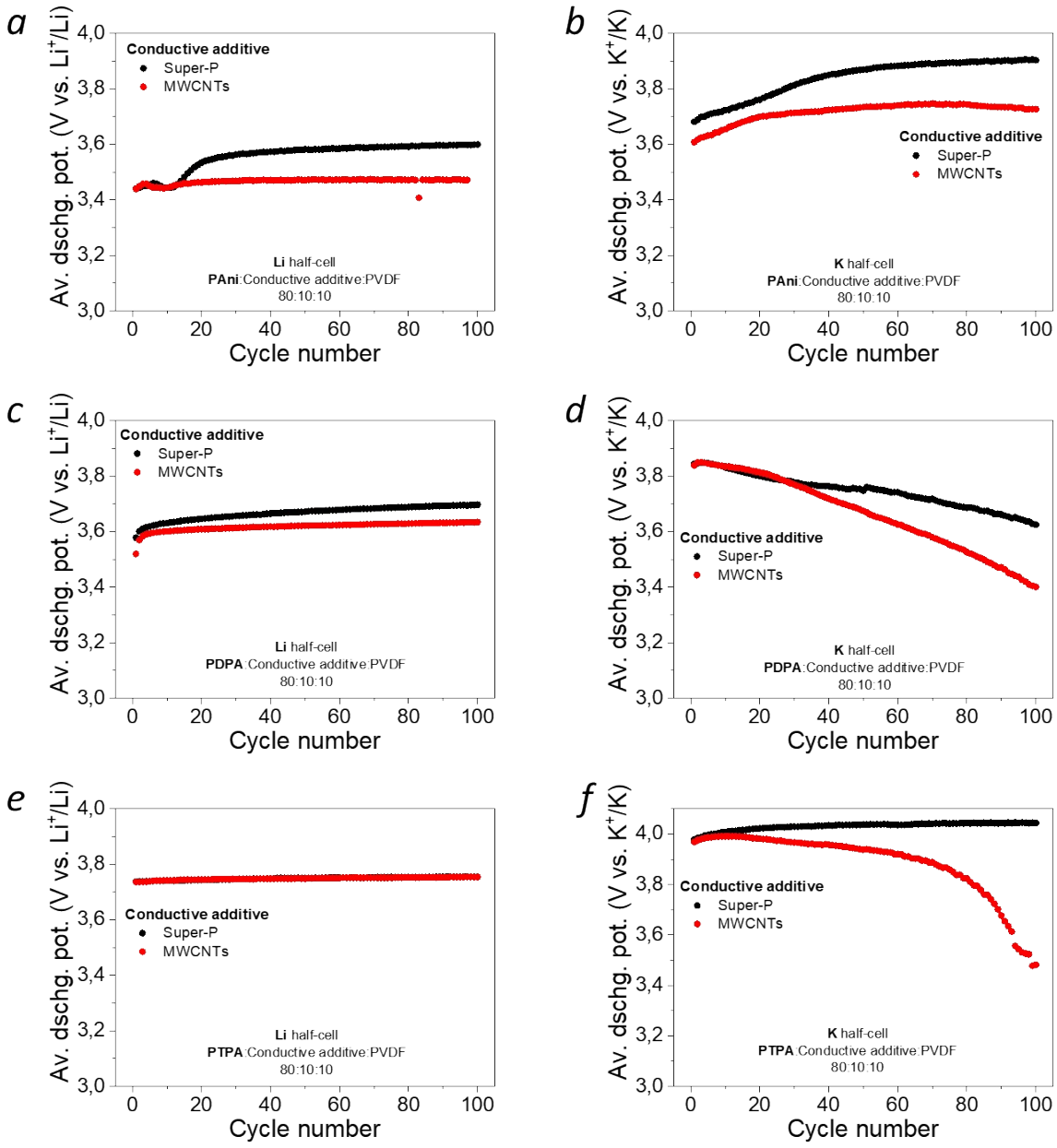

Figure S16. Evolution of the average discharge potentials of Li (a, c, e) and K (b, d, f) half-cells using the active material:conductive additive:PVDF (80:10:10) cathodes with PAni (a, b), PDPA (c, d) and PTPA (e, f) active materials.

Table S1. Assignment of signals in NMR spectra of N,N'-diphenylbenzidine (dimer) and PDPA (polymer). See the Figure S2 for spectra images and carbon atoms numbering.

Carbon atom no.	Chemical shift, ppm	
	Dimer[1]	polymer
1	143.32	141.01
2	142.01	141.01
3	131.52	129.54
4	129.12	126.68
5	126.44	124.73
6	119.67	119.93
7	117.13	115.79
8	116.75	115.79

Table S2. Experimental specific capacities and energy densities of reduced (discharged) forms of PAni, PDPA and PTPA measured for cathode compositions: active material:MWCNTs:PVDF (80:10:10) and calculated values for oxidized (charged) forms with PF_6^- anions.

Material	Specific capacity (mAh/g)		Energy density (Wh/kg)	
	Discharged	Charged (anion: PF_6^-)	Discharged	Charged (anion: PF_6^-)
PAni	131	51	453	175
PDPA	145	77	523	280
PTPA	91	57	338	211

Table S3. Comparison of the results obtained in this work with the selected literature data on the polymeric cathode materials for dual-ion batteries.

Entry[a)]	Active material	Cathode composition[b)]	Current density (mA/g)	Specific capacity (mAh/g)	Energy density (Wh/kg)	Realistic energy density (Wh/kg)	Average discharge potential (V)	Ref.
1 (This work)	**PDPA**	**AM:MWCNTs:PVDF (80:10:10)**	**100**	**145**	**523**	**418**	**3,61**	**-**
2 (10)	PTPA	AM:AB:PTFE (70:20:10)	50	103	387	271	3,76	2
3 (11)	p-DPPZ	AM:SP:PVDF (75:15:10)	105	150	530	398	3,53	3
4 (12)	Poly(Ph-PZ)-10	AM:SP+CMK3:PVDF (30:60:10)	1045	223	769	230	3,45	4
5 (12)	Poly(Ph-PZ)-10	AM:SP+CMK3:PVDF (60:30:10)	209	167	576	340	3,45	4
6 (13)	PHTPA	AM:AB:PVDF (40:50:10)	80	64	225	90	3,52	5
7 (13)	PHTPA	AM:AB+SWCNTs: PVDF (80:10:10)	80	67	235	188	3,51	5
8 (14)	PAni	AM:CB:PTFE (70:20:10)	10	138	415	291	3,01	6
9 (18)	PDPPD	AM:SP:PVDF (50:40:10)	105	102	362	181	3,55	7
10 (21)	PDPA-AQ	AM:AB:PVDF (40:50:10)	21	159	362	145	2,28	8
11 (22)	PTTPAB	AM:AB:PVDF (50:40:10)	20	86,7	327	164	3,77	9
12 (23)	PTDATA	AM:AB:PVDF (50:40:10)	20	133	410	205	3,08	10
13 (24)	PTPA-TEMPO	AM:AB:PVDF (50:40:10)	20	140	483	242	3,45	11
14 (25)	p-DPPZ	AM:SP:PVDF (50:40:10)	200	162	593	297	3,66	12
15 (26)	PTPA-NO2	AM:AB:PTFE (70:20:10)	40	72	259	18	3,60	13
16 (27)	Cu-TCA	AM:SP:PVDF (80:10:10)	73	102	297	238	2,91	14

a) The references specified in the Figure 5 and in the reference list of the main article text are given in the brackets;
b) The following acronyms were used: AM – active material, PVDF – polyvinylidene fluoride, PTFE – polytetrafluoroethylene, AB – acetylene black, CB – carbon black, SP – super-P carbon, SWCNTs – single-walled carbon nanotubes, MWCNTs – multi-walled carbon nanotubes, CMK3 – carbon mesostructures at KAIST – 3 (special type of carbon naterial); the materials content is given in the brackets.

Table S4. Comparison of the results obtained in this work with the selected literature data on the polymeric cathode materials for dual-ion batteries (continuation).

Entry[a)]	Active material	Cathode composition[b)]	Current density (mA/g)	Specific capacity (mAh/g)	Energy density (Wh/kg)	Realistic energy density (Wh/kg)	Average discharge potential (V)	Ref.
17 (28)	Poly-PPDA-PYR	AM:MWCNTs:PVDF (30:50:20)	20	113	360	108	3,19	15
18 (29)	PTPA	AM:MWCNTs:PVDF (65:25:10)	20	82	297	193	3,61	16
19 (30)	PTh	AM:CB:PTFE (85:10:5)	100	62	241	205	3,87	17
20 (31)	Poly(exTTF)	AM:VGCF:PVDF (10:80:10)	132	108	338	34	3,13	18
21 (32)	PV2T	AM:SP:PVDF (40:55:5)	110	105	411	16	3,91	19
22 (33)	PDDTB	AM:CB:PTFE (40:40:20)	50	363	712	285	1,96	20
23 (34)	PTVE	AM:VGCF:PTFE (20:70:10)	81	114	358	72	3,14	21
24 (35)	PPy-C-TEMPO	AM:AB:PVDF (50:40:10)	20	115	368	184	3,20	22
25 (36)	PTMA	AM(60%):SP:PVDF	111	79	271	163	3,43	23
26 (37)	PFFAL2	AM:VGCF:PVDF (10:80:10)	82	89	307	31	3,47	24
27 (38)	H-MPTN	AM:SP:PVDF (15:40:10)	50	80	255	59	3,19	25
28 (38)	H-MPTN-TCNE	AM:SP:PVDF (15:40:10)	50	146	408	94	2,79	25
29 (39)	SPTPA	AM:AB:PVDF (30:50:40)	200	93	335	84	3,60	26
30 (40)	PT-DMPD-10%	AM:SP:PVDF (30:60:10)	773	150	501	150	3,340	27
31 (40)	PT-DMPD-10%	AM:SP:PVDF (75:15:10)	773	132	453	340	3,43	27

a) The references specified in the Figure 5 and in the reference list of the main article text are given in the brackets;
b) The following acronyms were used: AM – active material, PVDF – polyvinylidene fluoride, PTFE – polytetrafluoroethylene, AB – acetylene black, CB – carbon black, SP – super-P carbon, MWCNTs – multi-walled carbon nanotubes, VGCF – vapor grown carbon fiber; the materials content is given in the brackets.

References

1 Spectral Database for Organic Compounds (SDBS), NMR spectrum, SDBS No.: 1731CDS-01-853, https://sdbs.db.aist.go.jp (accessed September 9, 2020).

2 J. K. Feng, Y. L. Cao, X. P. Ai and H. X. Yang, J. Power Sources, 2008, 177, 199–204.

3 G. Dai, X. Wang, Y. Qian, Z. Niu, X. Zhu, J. Ye, Y. Zhao and X. Zhang, Energy Storage Mater., 2019, 16, 236–242.

4 C. N. Gannett, B. M. Peterson, L. Shen, J. Seok, B. P. Fors and H. D. Abruña, ChemSusChem, 2020, 13, 2428–2435.

5 K. Yamamoto, D. Suemasa, K. Masuda, K. Aita and T. Endo, ACS Appl. Mater. Interfaces, 2018, 10, 6346–6353.

6 H. Gao, L. Xue, S. Xin and J. B. Goodenough, Angew. Chemie - Int. Ed., 2018, 57, 5449–5453.

7 F. A. Obrezkov, A. F. Shestakov, V. F. Traven, K. J. Stevenson and P. A. Troshin, J. Mater. Chem. A, 2019, 7, 11430–11437.

8 W. Huang, T. Jia, G. Zhou, S. Chen, Q. Hou, Y. Wang, S. Luo, G. Shi and B. Xu, Electrochim. Acta, 2018, 283, 1284–1290.

9 Z. Chen, W. Li, Y. Dai, N. Xu, C. Su, J. Liu and C. Zhang, Electrochim. Acta, 2018, 286, 187–194.

10 C. Su, H. He, L. Xu, K. Zhao, C. Zheng and C. Zhang, J. Mater. Chem. A, 2017, 5, 2701–2709.

11 C. Su, F. Yang, L. Xu, X. Zhu, H. He and C. Zhang, Chempluschem, 2015, 80, 606–611.

12 F. A. Obrezkov, V. Ramezankhani, I. Zhidkov, V. F. Traven, E. Z. Kurmaev, K. J. Stevenson and P. A. Troshin, J. Phys. Chem. Lett., 2019, 10, 5440–5445.

13 L. Zhu and X. Cao, Int. J. Electrochem. Sci., 2015, 10, 4359–4365.

14 Z. Peng, X. Yi, Z. Liu, J. Shang and D. Wang, ACS Appl. Mater. Interfaces, 2016, 8, 14578–14585.

15 C. J. Yao, J. Xie, Z. Wu, Z. J. Xu, S. Zhang and Q. Zhang, Chem. - An Asian J., 2019, 14, 2210–2214.

16 C. Su, Y. Ye, X. Bu, L. Xu and C. Zhang, Adv. Mater. Res., 2011, 336, 1512–1515.

17 L. Liu, F. Tian, X. Wang, Z. Yang, M. Zhou and X. Wang, React. Funct. Polym., 2012, 72, 45–49.

18 B. Häupler, R. Burges, C. Friebe, T. Janoschka, D. Schmidt, A. Wild and U. S. Schubert, Macromol. Rapid Commun., 2014, 35, 1367–1371.

19 A. Wild, M. Strumpf, B. Häupler, M. D. Hager and U. S. Schubert, Adv. Energy Mater., 2017, 7, 1601415.

20 J. Y. Zhang, L. B. Kong, L. Z. Zhan, J. Tang, H. Zhan, Y. H. Zhou and C. M. Zhan, J. Power Sources, 2007, 168, 278–281.

21 M. Suguro, S. Iwasa, Y. Kusachi, Y. Morioka and K. Nakahara, Macromol. Rapid Commun., 2007, 28, 1929–1933.

22 L. Xu, F. Yang, C. Su, L. Ji and C. Zhang, Electrochim. Acta, 2014, 130, 148–155.

23 J. K. Kim, G. Cheruvally, J. H. Ahn, Y. G. Seo, D. S. Choi, S. H. Lee and C. E. Song, J. Ind. Eng. Chem., 2008, 14, 371–376.

24 J. Xiang, R. Burges, B. Haupler, A. Wild, U. S. Schubert, C.-L. Ho and W.-Y. Wong, Polymer (Guildf)., 2015, 68, 328–334.

25 J. Choi, E. S. Kim, J. H. Ko, S. M. Lee, H. J. Kim, Y.-J. Ko and S. U. Son, Chem. Commun., 2017, 53, 8778–8781.

26 C. Zhang, X. Yang, W. Ren, Y. Wang, F. Su and J. Jiang, J. Power Sources, 2016, 317, 49–56.

27 B. M. Peterson, D. Ren, L. Shen, Y. C. M. Wu, B. Ulgut, G. W. Coates, H. D. Abruna and B. P. Fors, ACS Appl. Energy Mater., 2018, 1, 3560–3564.